Zhi et al., Fig. S1

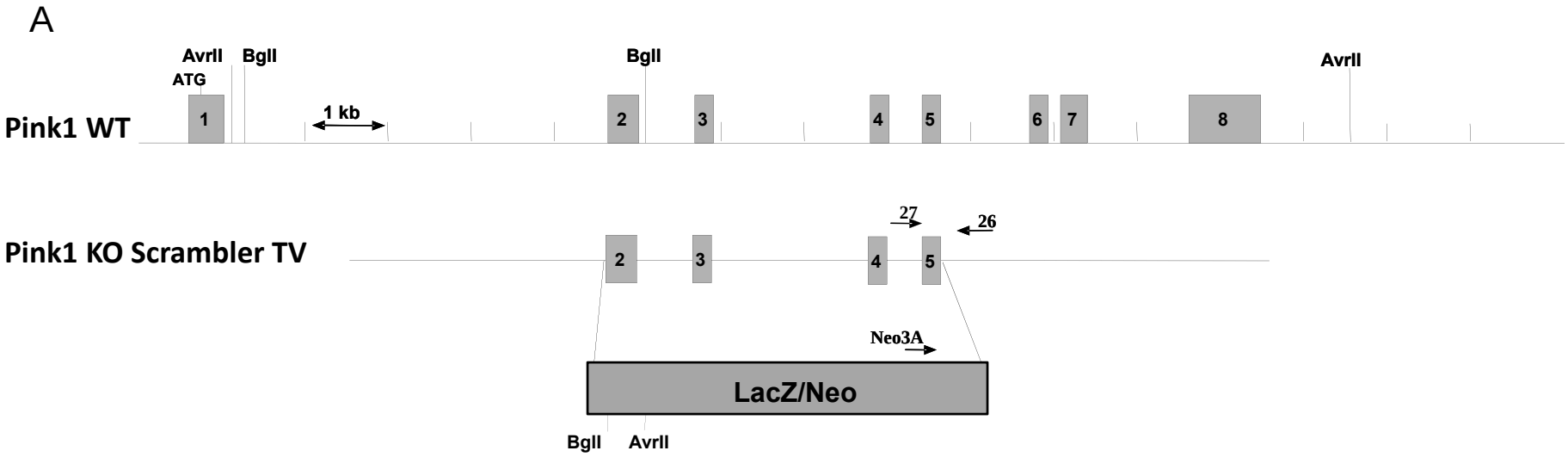

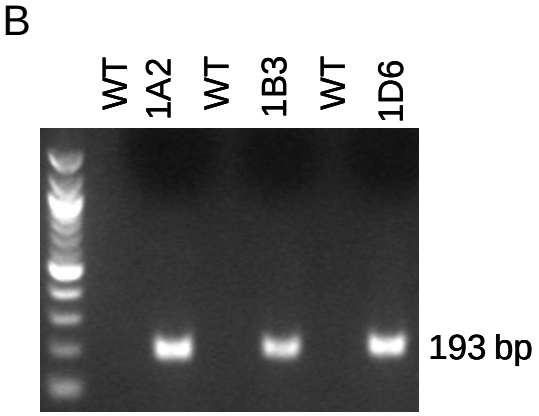

CCTTCTTGACGAGTTCTTCTGAGGGGATCGGCAAT
AAAAAGACAGAATAAAACGCACGGGTGTTGGGTC
GTTTGTTCGGATCCGAATTCCTCGAGGGCGCGCC
ATTTAAATGGCCAGCGAGGCCACACACCCAGAGT
GCTCCAAGAAGGGGCATTAGAGACCCTGAGGGC

Red: Part of Neo Cassette Sequence

Blue: Part of PINK1 gene 5th intron sequence

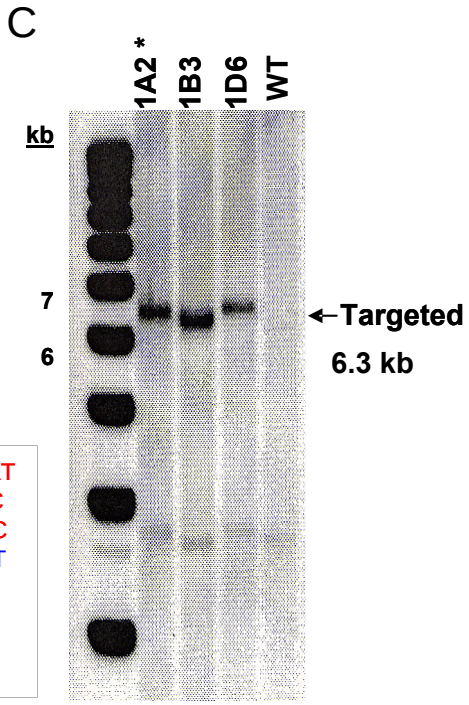

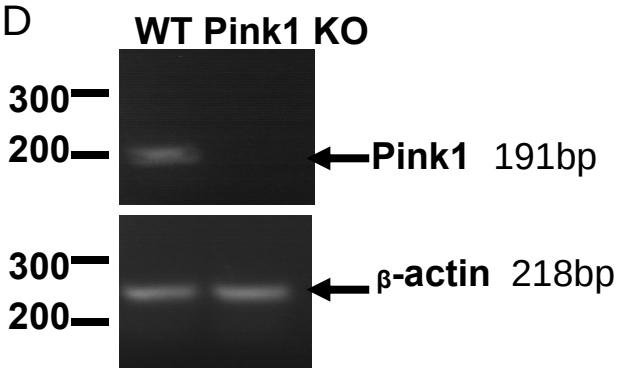

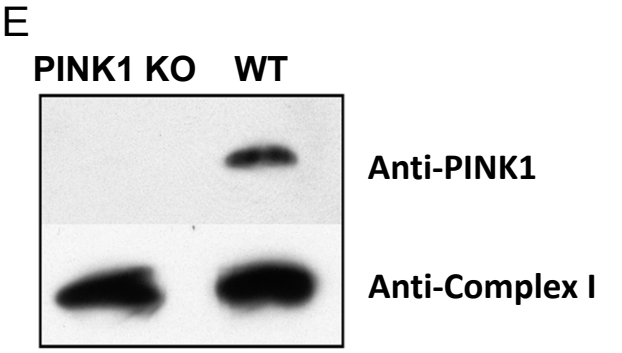

Zhi et al., Fig. S2

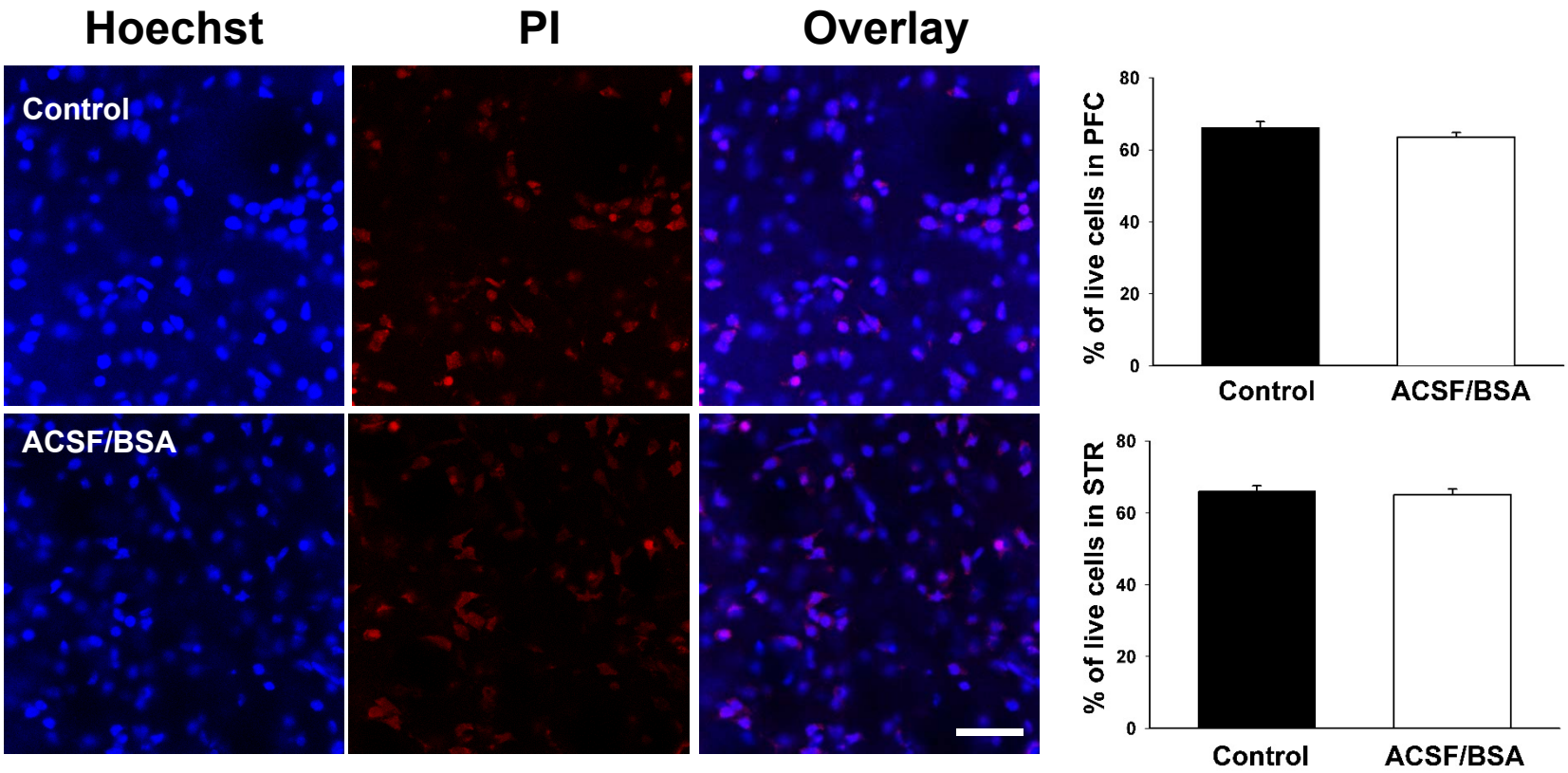

Zhi et al., Fig. S3

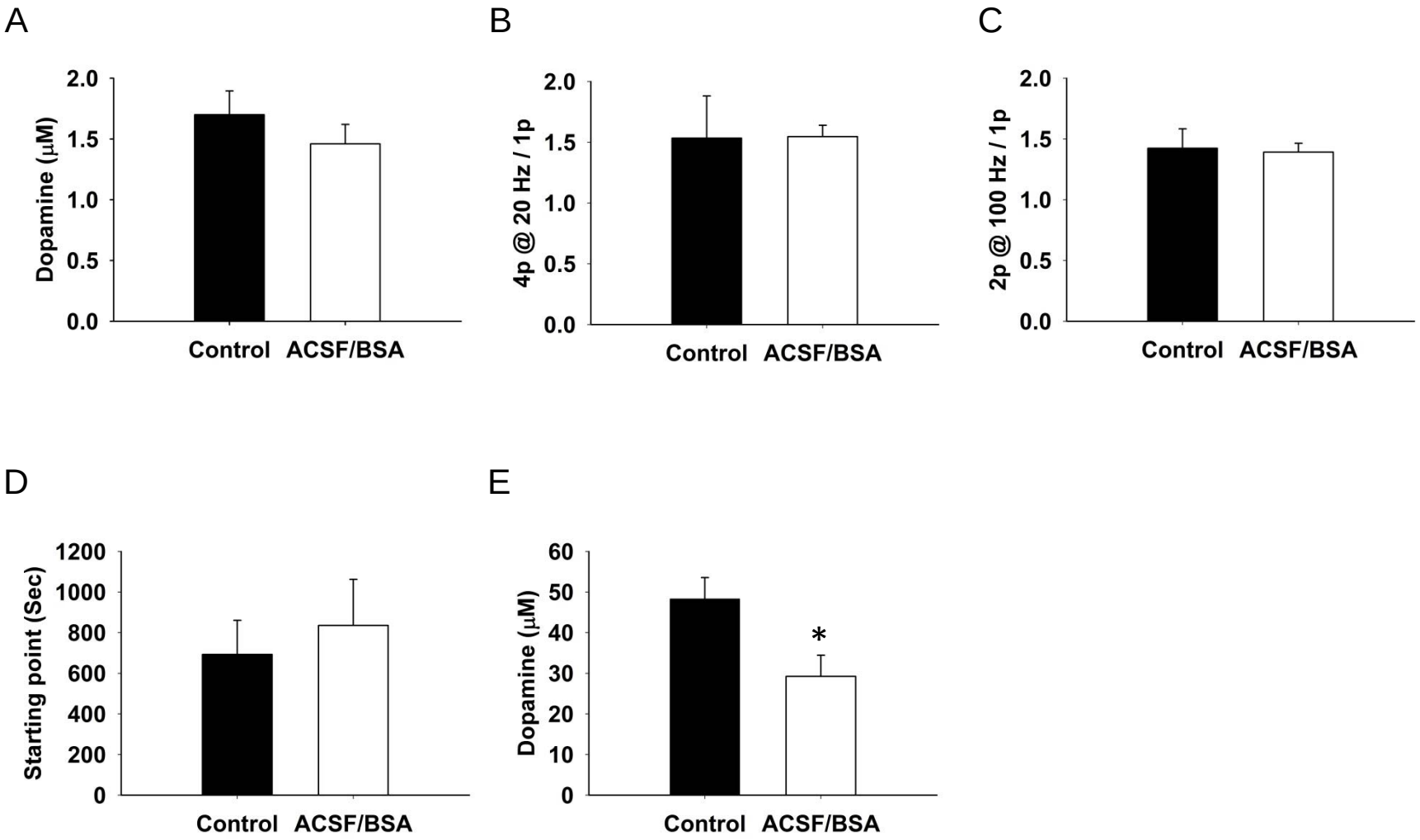

Zhi et al., Fig. S4

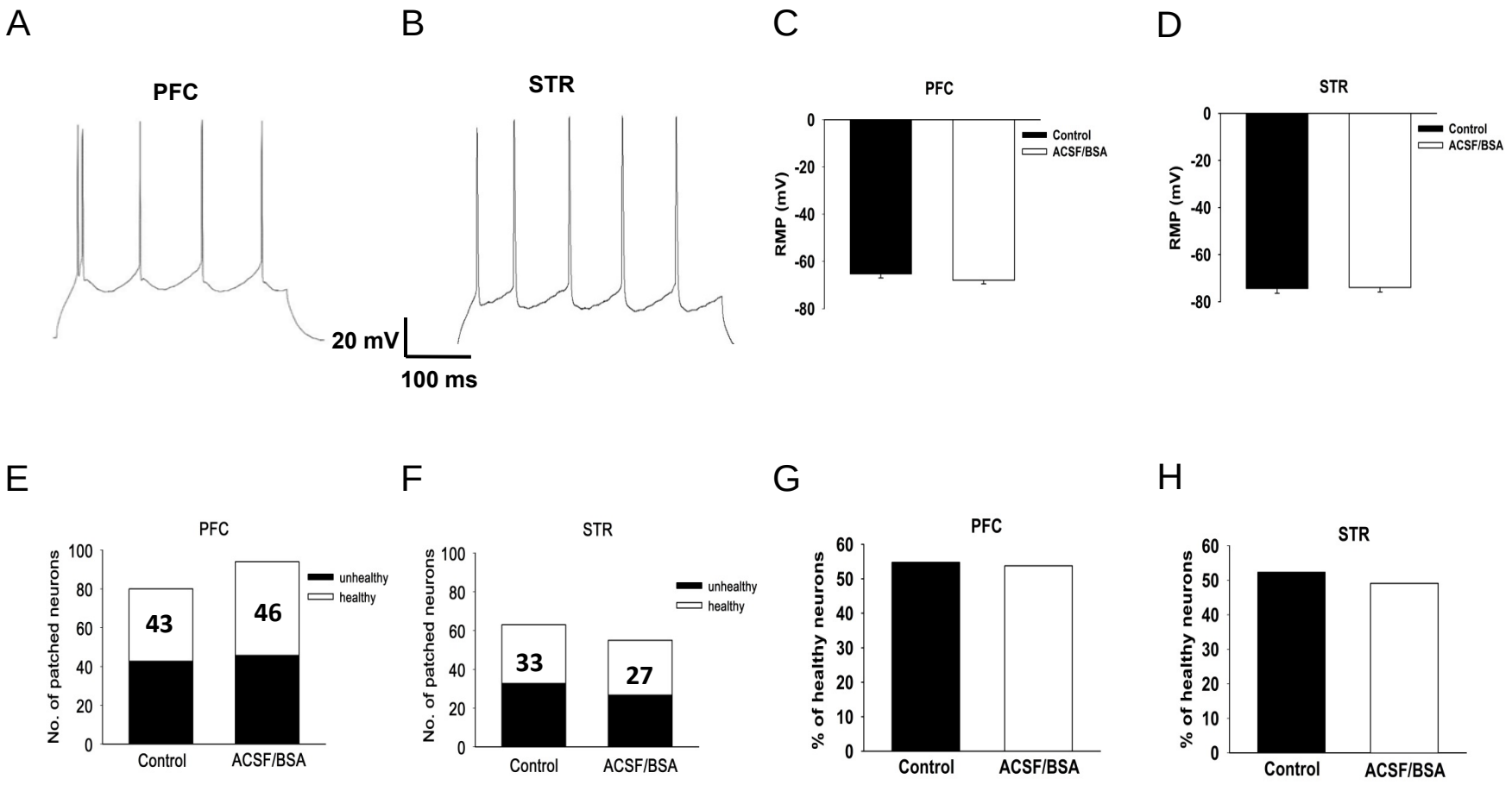

Zhi et al., Fig. S5

A

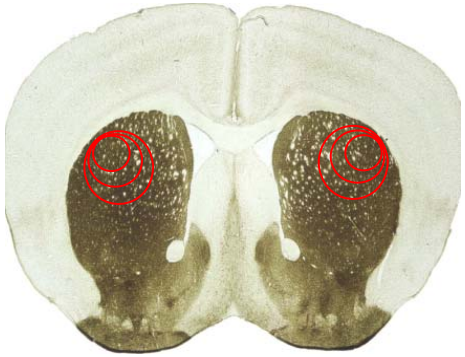

C

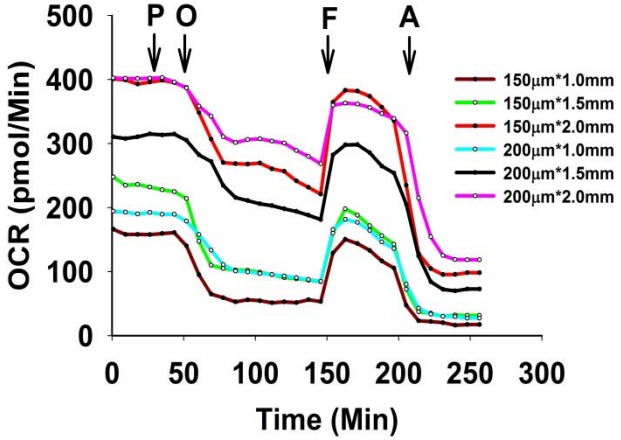

E

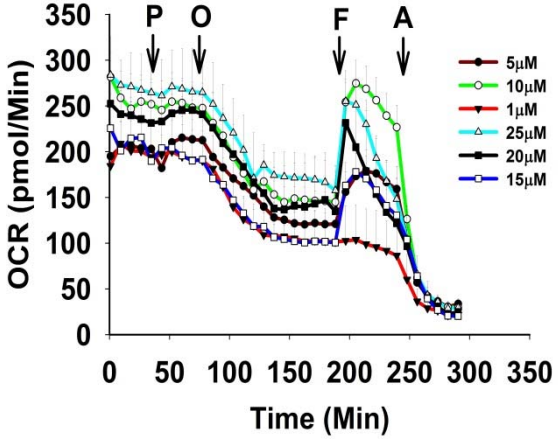

B

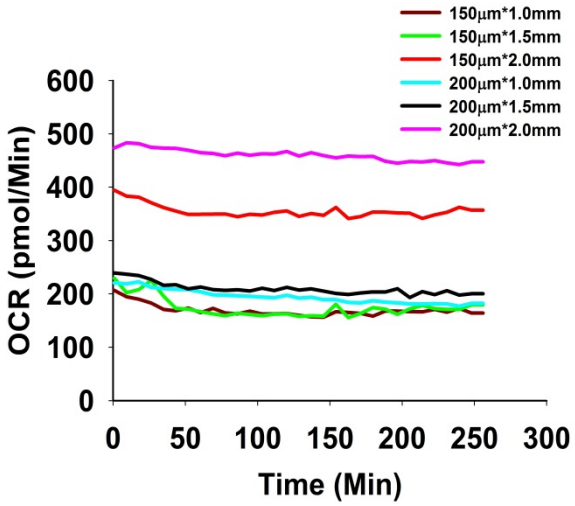

D

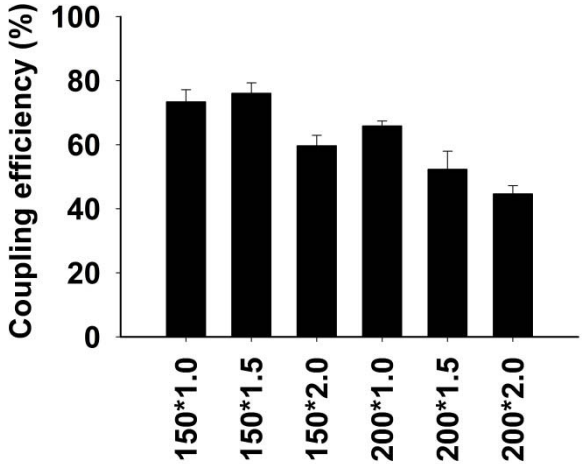

Supplementary Information

Fig. S1. Generation of Pink1 KO mice

(A) Targeting strategy of PINK1 knockout mice: exons 2-5 in PINK1 gene was designed to deleted by gene-targeting, so that the majority of the kinase domain was removed. (B) PCR and sequence confirmation of the correct targeting: Primers Neo3A and 26 were used for PCR of mouse tail DNAs. The 193 bp PCR products specific to targeted alleles were sequenced to validate the correct targeting event. (C) Confirmation of specific targeting to the PINK1 locus by genomic Southern blot. A signal of the expected size was detected by neo probe in all PINK1 mice but not in WT mice. The asterisk marked mouse was used for further breeding, and their offspring genomic PINK1 locus was sequenced to confirm correct targeting. (D) RT-PCR analysis of PINK1 mRNA level in Pink1 KO mouse: images of electrophoretic gel for RT-PCR products of Pink1 (the top band) and internal control β-actin (the lower band) from Pink1 KO and WT mice. (E) Antibody against PINK1 confirmed that PINK1 protein was absent in homozygous PINK1 KO mice. (WT: wild type mice; 1A2, 1B3, 1D6: heterozygous founders of $PINK1^{+/-}$ genotype)

Fig. S2. Propidium iodide labeling shows same live cells in ACSF/BSA group in both PFC and STR slices

150 μm striatal slices were prepared as ACSF/BSA and control group. The percentage of live cells in both PFC and STR were analyzed using PI (10 μM) and Hoechst 33258 (10 μM) double labeling, followed by confocal imaging at 60 μm beneath the surface and cell number counting (Hoechst 33258 labels all the cells whereas PI only labels live cells) (N = 3, n = 8). No significant difference was observed between ACSF/BSA group and control for both PFC and

STR area. Representative images were from STR area, scale bar: 50 μm.

Fig. S3. Comparison of DA release in ACSF/BSA group and control group

150 μm striatal slices from both ACSF/BSA and control group were measured for DA release to evaluate the health of slices. No significant difference of 1p-evoked DA release (A) or train-pulse-evoked DA release (B) was observed between ACSF/BSA group and control group. The ratio of 2 pulses at 100Hz to single pulse which indicates DA release probability was not significantly different either (C). No significant difference for the starting point of FCCP-induced DA massive release for ACSF/BSA group and control group (D), whereas the massive DA release was decreased in ACSF/BSA group (E).

Fig. S4. The percentage of healthy neurons in the PFC and STR is not significantly altered in ACSF/BSA group when compared to control

The health of both pyramidal neurons in the PFC and MSNs in the STR were evaluated using patch clamp recording. The neuron was determined as healthy, if there was stable action potential firing during the current-injected depolarization phase (A and B); otherwise, the neuron was determined unhealthy. The resting membrane potential (RMP) was nearly the same in ASCF/BSA group and control (C and D). More than 80 pyramidal neurons (E) and 55 MSN neurons (F) were patched for analysis and the percentage of healthy neurons was not different in both PFC (g, 61.2 % *vs.* 57.5 %) and STR (h, 57.1 % *vs.* 49.0 %).

Fig. S5. Optimal striatial slice condition for seahorse XF24 flux respiration assay

Diagram of tissue punch sizes (1.0 mm, 1.5 mm, and 2.0 mm in diameter) for STR with circles

representing the areas that were obtained for STR analysis for STR. (A) O2 consumption rates (OCRs) for different thickness and punch size of slice in control group showed stable basal respiration over the whole measurement, and OCR was proportional to the volume of slice. (B) OCRs were measured in 150 μm and 200 μm thickness slices punched by 1.0 mm, 1.5 mm, and 2.0 mm puncher respectively. (C, D) With 10 mM pyruvate (P), 20 μM Oligomycin (O), 10 μM FCCP (F), and 20 μM Antimycin A (A) injected sequentially, the mitochondria coupling efficiency was compared among different groups, and 150 μm * 1.5 mm seems the best of all conditions.